SutA is a bacterial transcription factor expressed during slow growth in *Pseudomonas aeruginosa*

Brett M. Babin[a,1], Megan Bergkessel[b,c,d,1], Michael J. Sweredoski[e], Annie Moradian[e], Sonja Hess[e], Dianne K. Newman[b,c,d,2], and David A. Tirrell[a,2]

[a]Division of Chemistry and Chemical Engineering, California Institute of Technology, Pasadena, CA 91125; [b]Division of Geological and Planetary Sciences, California Institute of Technology, Pasadena, CA 91125; [c]Division of Biology and Biological Engineering, California Institute of Technology, Pasadena, CA 91125; [d]Howard Hughes Medical Institute, California Institute of Technology, Pasadena, CA 91125; and [e]Proteome Exploration Laboratory, Beckman Institute, California Institute of Technology, Pasadena, CA 91125

Edited by Lucia B. Rothman-Denes, The University of Chicago, Chicago, IL, and approved December 17, 2015 (received for review July 21, 2015)

Microbial quiescence and slow growth are ubiquitous physiological states, but their study is complicated by low levels of metabolic activity. To address this issue, we used a time-selective proteome-labeling method [bioorthogonal noncanonical amino acid tagging (BONCAT)] to identify proteins synthesized preferentially, but at extremely low rates, under anaerobic survival conditions by the opportunistic pathogen *Pseudomonas aeruginosa*. One of these proteins is a transcriptional regulator that has no homology to any characterized protein domains and is posttranscriptionally upregulated during survival and slow growth. This small, acidic protein associates with RNA polymerase, and chromatin immunoprecipitation (ChIP) followed by high-throughput sequencing suggests that the protein associates with genomic DNA through this interaction. ChIP signal is found both in promoter regions and throughout the coding sequences of many genes and is particularly enriched at ribosomal protein genes and in the promoter regions of rRNA genes. Deletion of the gene encoding this protein affects expression of these and many other genes and impacts biofilm formation, secondary metabolite production, and fitness in fluctuating conditions. On the basis of these observations, we have designated the protein SutA (survival under transitions A).

Pseudomonas aeruginosa | slow growth | transcription | proteomics | BONCAT

The cosmopolitan bacterium *Pseudomonas aeruginosa* is notorious as an opportunistic pathogen of burn wounds, medical devices, and the lungs of cystic fibrosis (CF) patients. The bacterium's genome is large and encodes an unusually high proportion of regulators (1). Compared with *Escherichia coli*, *P. aeruginosa* possesses more σ factors that direct RNA polymerase (RNAP) to promoter regions (24 vs. 7), more DNA-binding activators and repressors that enhance or prevent RNAP binding and transcription (~550 vs. 150) (2, 3) and more small, noncoding RNAs (ncRNAs) that modulate the stability or translation of target transcripts (200 vs. 100) (4, 5). Much effort has been directed toward understanding the mechanisms by which this regulatory capacity governs the behaviors—such as quorum sensing, protein secretion, secondary metabolite production, and biofilm formation—that contribute to *P. aeruginosa* virulence.

The physiological states of bacteria involved in chronic infections are substantially different from those most often studied in standard laboratory experiments; chronic infections are characterized by slow growth rates imposed by limited nutrients or oxidants or by host immune responses. Direct measurements of in situ microbial growth rates in the context of lung infections in CF patients have revealed doubling times of several days (6). Measurements of expectorated sputum show that hypoxic and anoxic zones exist within infected CF airways and can experience dramatic fluctuations in redox potential (7); *P. aeruginosa* strains isolated from the CF lung show gene expression patterns consistent with adaptations to hypoxia (8), suggesting that a lack of oxygen may limit growth. Although *P. aeruginosa* can generate energy in this environment by using nitrate as the terminal electron acceptor for respiration (9), levels of nitrate may be too low or too variable for nitrate respiration to represent the sole energy source in anoxic zones. *P. aeruginosa* can also remain viable for weeks in an anaerobic survival state by carrying out substrate-level phosphorylation to generate ATP, using either pyruvate [assisted by phenazines (10)] or arginine as a carbon and energy source (11, 12). The cells do not grow when limited to this type of metabolism, and little is known about how basic cellular processes are maintained.

We explored the *P. aeruginosa* anaerobic survival state by identifying the proteins that are synthesized in this energy-limited condition. Previous studies have characterized transcriptomic responses to low oxygen (13, 14) and have identified a few proteins that increase in abundance under conditions of anaerobic survival (15). The potential for important posttranscriptional regulation under stress conditions (16, 17) led us to take a proteomic approach, and the low metabolic rates that occur during anaerobic survival meant that the quantity of protein made after the shift to anaerobic conditions would likely be small relative to the size of the preexisting proteome. To address these challenges and specifically identify proteins associated with the anaerobic survival state, we used a time-selective proteome-labeling approach, referred to as bioorthogonal noncanonical amino acid tagging (BONCAT) (18, 19)

Significance

Pathogens that are dormant or growing slowly play important roles in chronic infections, but studying how cells adapt to these conditions is difficult experimentally. This work demonstrates that time-selective analysis of cellular protein synthesis, using bioorthogonal noncanonical amino acid tagging (BONCAT), can provide the sensitivity needed to identify important factors in slow-growth physiology. We identified in *Pseudomonas aeruginosa*, a previously uncharacterized transcriptional regulator that is expressed preferentially under slow-growth conditions, binds RNA polymerase, and has widespread effects on gene expression. This factor is one of several proteins of unknown function identified in our proteomic analysis, and our results suggest that further characterization of fundamental cellular processes under these conditions will shed light on important and understudied realms of biology.

Author contributions: B.M.B., M.B., M.J.S., A.M., S.H., D.K.N., and D.A.T. designed research; B.M.B. and M.B. performed research; B.M.B., M.B., M.J.S., S.H., D.K.N., and D.A.T. analyzed data; and B.M.B., M.B., M.J.S., S.H., D.K.N., and D.A.T. wrote the paper.

The authors declare no conflict of interest.

This article is a PNAS Direct Submission.

Data deposition: The data reported in this paper have been deposited in the Gene Expression Omnibus (GEO) database, www.ncbi.nlm.nih.gov/geo (accession no. GSE66181).

[1]B.M.B. and M.B. contributed equally to this work.

[2]To whom correspondence may be addressed. Email: dkn@caltech.edu or tirrell@caltech.edu.

This article contains supporting information online at www.pnas.org/lookup/suppl/doi:10.1073/pnas.1514412113/-/DCSupplemental.

to enrich and identify proteins made during anaerobic survival. We identified 91 proteins that were preferentially synthesized under anaerobic survival conditions compared with aerobic growth conditions in the same medium. Phenotypic screens of mutants lacking these proteins led us to focus on a single uncharacterized protein that is expressed under multiple slow-growth conditions and plays a role in biofilm formation, virulence factor production, and survival under transitions between different conditions. We used a combination of coimmunoprecipitation (co-IP), mass spectrometry, and sequencing to establish this protein as a transcriptional regulator. The protein binds RNA polymerase, causes widespread changes in gene expression, and plays a direct role in the regulation of genes encoding ribosomal components.

Results

BONCAT Enables Enrichment and Identification of Proteins Synthesized at Low Rates During Anaerobic Survival. The BONCAT technique relies on pulse-labeling cultures with the methionine (Met) surrogate L-azidohomoalanine (Aha) (Fig. S1*A*), which is incorporated into nascent proteins by a cell's endogenous translational machinery. Aha provides a chemical handle by which newly synthesized proteins can be distinguished and physically enriched from the prepulse proteome (Fig. S1*B*). To probe protein synthesis during anaerobic survival on arginine, we shifted an aerobic arginine culture to anaerobic conditions, allowed cells to adapt for 24 h, and then treated them with Aha (Fig. 1*A*). The total amount of incorporation of Aha into cellular protein during a 16-h pulse was approximately fourfold lower than that observed for an aerobic sample treated for only 15 min (Fig. 1*B* and Fig. S1 *C* and *D*), providing evidence of slow, but detectable, protein synthesis during anaerobic survival. Lysates from anaerobic and aerobic cultures were treated with an alkyne-biotin affinity tag, enriched for Aha-labeled proteins with streptavidin beads (Fig. S1*F*), and analyzed by liquid chromatography–tandem mass spectrometry (LC-MS/MS).

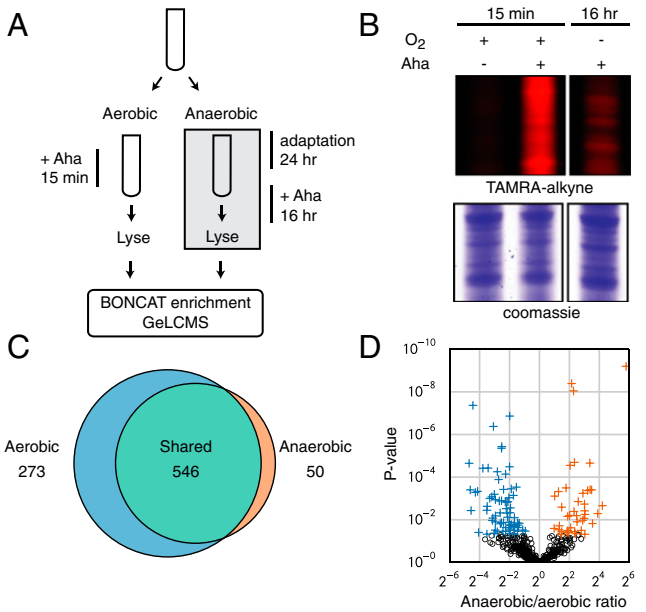

Fig. 1. BONCAT enables enrichment and identification of proteins synthesized during anaerobic survival. (*A*) Overall scheme of the BONCAT experiment. (*B*) Lysates were treated with tetramethylrhodamine (TAMRA)-alkyne and separated via SDS/PAGE to visualize Aha incorporation. Coomassie staining indicates total protein loading (see Fig. S1*E* for entire gel). (*C*) Identified proteins fell into three groups: unique to the aerobic sample, shared, and unique to the anaerobic sample. (*D*) Protein ratios between the two samples were calculated via label-free quantification. Proteins significantly more abundant in each sample (Benjamini–Hochberg false-discovery rate, $P < 0.05$) are marked with crosses.

We identified 869 proteins overall; 50 were detected only in the anaerobic sample, and 273 were detected only in the aerobic sample (Fig. 1*C*). For the 546 proteins identified in both samples, we used label-free quantification to find proteins preferentially synthesized under each set of conditions. Peptide intensities were normalized to the total peptide intensity for each run, and the ratio for each protein was calculated as the median of its peptide ratios. We found 41 and 74 proteins whose anaerobic:aerobic ratios were significantly greater than or less than 1, respectively (Fig. 1*D*). Complete proteomic results are listed in Dataset S1. The 91 proteins that were more abundant or detected only in the anaerobic sample included proteins previously implicated in anaerobic growth or survival, such as targets of the oxygen-sensing regulator Anr: NirM, CcpR, PctA, PA14_06000, and the universal stress protein UspK (14, 15). More than one-third of the proteins, however, are annotated as "hypothetical proteins." We hypothesized that this list of "anaerobic hits" might contain poorly characterized proteins that play important roles in regulating slow-growth physiology. To identify general regulators, we tested the ability of transposon mutants of these genes [from a mutant library (20)] to form biofilms—another growth condition in which nutrients and oxygen are limited and cells experience low metabolic rates (21).

We looked for defects in two modes of biofilm growth: as attached biofilms on a polystyrene substrate and as colony biofilms on agar plates (Fig. S2 *A* and *B*). Mutants for three genes showed defects in both biofilm assays: the pilus assembly protein FimV and hypothetical proteins PA14_44460 and PA14_69770. FimV and PA14_44460 have previously been implicated as contributors to type II secretion—a process known to be important for biofilm formation (22). In contrast, PA14_69770 has no homology to any characterized proteins or domains and has not been investigated to date. For this reason, we chose to study further the role of PA14_69770 in *P. aeruginosa* under survival and slow-growth conditions. Based on its contribution to fitness during transitions to and from these states, uncovered in our studies, we refer to this protein as SutA (survival under transitions A).

SutA Promotes Biofilm Formation, Inhibits Pyocyanin Production, and Confers a Fitness Advantage Under Fluctuating Conditions. We generated a clean deletion strain (Δ*sutA*) and an arabinose-inducible overexpression strain (P_{ara}:*sutA*) to verify the results of the biofilm phenotype screens. Arabinose cannot support growth of *P. aeruginosa* when supplied as the sole carbon source and so does not act as a nutrient during induction of gene expression in this context. For all experiments involving arabinose-induced overexpression, arabinose was also added to the wild-type and Δ*sutA* strains to control for any potential physiological impacts. The deletion mutant formed smooth colony biofilms that lacked the complex wrinkled structures observed in wild-type biofilms, whereas the overexpression strain did not show substantially different colony morphology (Fig. 2*A*). The deletion strain also formed smaller biofilms, and the overexpression strain larger biofilms, on polystyrene compared with the wild type (Fig. 2*B*). The biofilm deficiencies of the mutant strain were not attributable to a growth defect, because there were no differences in growth rates between Δ*sutA* and the wild-type strain during aerobic planktonic culture in either rich or minimal media (Fig. S2*C*). There was, however, a strong effect of SutA on the colors of planktonic cultures; Δ*sutA* cultures were more blue and P_{ara}:*sutA* cultures less blue than the wild type. This effect was pronounced under nutrient-poor conditions, following aerobic growth in minimal medium containing pyruvate as a carbon source (Fig. 2*C*). The blue color of high-density *P. aeruginosa* cultures is often attributable to the presence of the redox-active phenazine pyocyanin (PYO), which plays roles in signaling and virulence and whose production is sensitive to various regulatory inputs (23–25). We measured the concentrations of PYO and its metabolic precursor

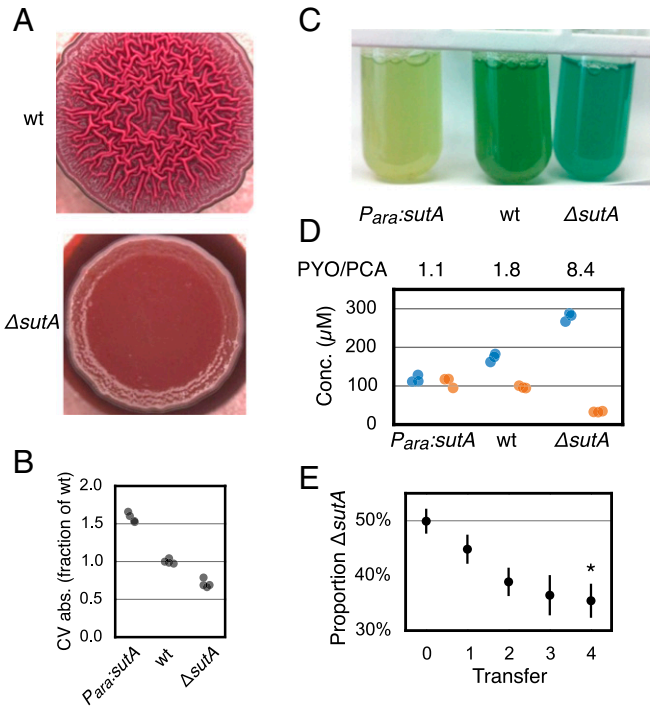

Fig. 2. Phenotypic characterization of *sutA* mutants. (*A*) Colony biofilms were grown for 6 d at room temperature. (*B*) Biofilm growth on polystyrene was measured with the crystal violet assay ($n = 4$). (*C*) Cultures were grown in pyruvate minimal medium to stationary phase overnight at 37 °C. (*D*) Concentrations of PYO (blue) and PCA (orange) in culture supernatants were measured via HPLC. Average molar ratios are indicated above the plot ($n = 3$). (*E*) Cocultures of wild-type and *ΔsutA* strains were subjected to repeated rounds of anaerobic survival followed by outgrowth to midexponential phase in LB. After each outgrowth, the proportion of *ΔsutA* was measured by fluorescence microscopy. Error bars show SE ($n = 6$). The asterisk indicates a significant difference from the initial time point (paired Student's *t* test, $P < 0.05$).

phenazine-1-carboxylic acid (PCA) in culture supernatants using HPLC and found that *ΔsutA* produced more PYO and less PCA than the wild type, whereas P_{ara}*:sutA* showed the opposite effect (Fig. 2*D*). Absorbance measurements of culture supernatants gave the same results (Fig. S2*D*).

Because control of biofilm formation and phenazine production relies on integration of multiple regulatory inputs, particularly those related to changes in cell density and nutrient availability, we tested SutA's contribution to the fitness of cells exposed to changing conditions. To detect subtle effects, we competed fluorescently marked wild-type and *ΔsutA* strains while they alternated between aerobic growth in Luria–Bertani (LB) and anaerobic survival in minimal arginine medium. On average, the wild-type strain significantly outcompeted *ΔsutA* after four transitions (Fig. 2*E*), and in five out of six trials, the wild-type strain showed a clear advantage after two transitions (Fig. S2*E*), suggesting that SutA is important during transitions to and from the survival state.

SutA Up-Regulation During Slow Growth Is Posttranscriptional. We initially focused on SutA based on its up-regulation under anaerobic survival conditions, but its roles in biofilm formation and phenazine production under aerobic conditions suggested that its expression is not solely dependent on anoxia. To assay SutA expression at both the transcript and protein levels, we generated a reporter strain carrying a fusion of the *sutA* promoter, 5′ untranslated region (UTR), and 3′ UTR to *gfp* (P_{sutA}*:gfp*). Both 5′ and 3′ UTRs have previously been shown to impact transcript stability and translation (26), so our construct was designed to capture effects conferred by both regions. We measured GFP fluorescence per cell using flow cytometry during growth in LB and pyruvate minimal media, starting in midexponential phase (which takes longer to reach in pyruvate minimal media than in LB). In LB, reporter protein levels per cell were low during mid- and late-exponential phase (0–3 h) but increased up to eightfold in late-stationary phase, whereas transcript levels (shown normalized to the level measured at time 0 in LB) varied less than twofold throughout the experiment (Fig. 3, solid lines). In pyruvate medium, in which cells grow approximately fourfold slower compared with LB and remain in exponential phase for a longer time (0–14 h) (see also Fig. S2*C*), GFP fluorescence per cell was higher than in LB during exponential growth and increased slightly with culture density before decreasing in late-stationary phase. As in LB, normalized transcript levels showed little variation (Fig. 3, dashed lines).

To verify that changes in fluorescence measurements reflected regulation of transcription and translation and were not attributable to accumulation of GFP, we constructed an analogous reporter that encoded a fusion of the promoter, 5′ UTR, and 3′ UTR of the ribosomal protein gene *rpsG* to *gfp* (P_{rpsG}*:gfp*). As expected, per-cell GFP expression was high in exponential phase and decreased sevenfold in stationary phase (Fig. S2 *F–H*). In

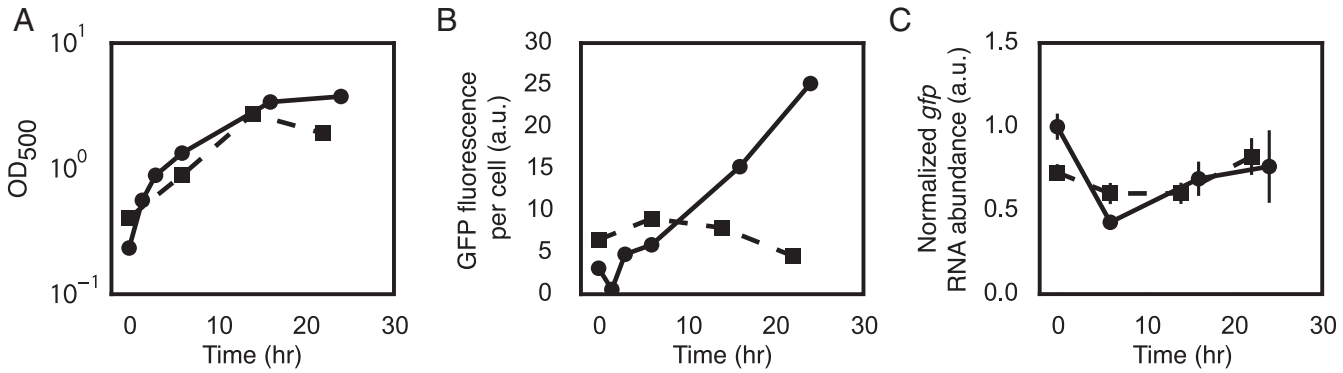

Fig. 3. SutA up-regulation during slow growth is posttranscriptional. A P_{sutA}*:gfp* cassette was transposed into a neutral locus of the wild-type strain. Optical density at 500 nm (*A*), per-cell GFP fluorescence (*B*), and *gfp* transcript abundance (*C*) were measured throughout growth in LB (circles and solid lines) and pyruvate minimal medium (squares and dashed lines). Error bars represent the SE of biological replicates ($n = 3$) and, in some cases, are smaller than the marker. RNA abundances were normalized by the housekeeping gene *oprI*. RNA and GFP measurements are relative to the value for the P_{sutA}*:gfp* strain in LB at time 0.

contrast to the *sutA* reporter construct, transcript and protein levels followed the same trend.

These results indicate that SutA up-regulation occurs in conditions that cause slow growth and does not require a lack of oxygen. Because slow growth in pyruvate minimal medium resulted in constitutive moderate expression of SutA and because we could clearly observe a phenazine phenotype resulting from *sutA* mutation in this medium, we chose to use late-exponential phase in pyruvate minimal medium for further study of the functions of SutA.

SutA Interacts with RNA Polymerase. To gain insight into how SutA brings about the observed phenotypic changes, we sought to identify interacting protein partners. We generated an N-terminal hemagglutinin (HA)-tagged copy of SutA (HA-SutA) and verified that expression of this protein from the pMQ72 plasmid backbone in the Δ*sutA* background complemented the phenazine (Fig. 4*A*) and biofilm (Fig. 4*B*) phenotypes. We performed an immunoprecipitation (IP) against the HA epitope in this strain and in the Δ*sutA* strain carrying the empty pMQ72 vector following induction with arabinose in late-exponential phase in pyruvate minimal medium. We identified coprecipitating proteins via LC-MS/MS analysis of the eluent fraction. Proteins coprecipitated with HA-SutA or from the empty vector control were digested with trypsin and reacted with "medium" or "light" dimethyl labels, respectively. Peptides from both IPs were mixed and ratios directly quantified by LC-MS/MS. In two experiments, we identified three proteins that were enriched at least fivefold in the strain expressing HA-SutA compared with the empty vector control: the α, β, and β′ subunits of RNAP (RpoA, RpoB, and RpoC) (Fig. 4*C*). We also detected coprecipitation of RpoA with HA-SutA in the IP eluent fraction by Western blot (Fig. 4*D*). The presence of some RpoA signal in the unbound ("FT") fraction suggests that not all cellular RNAP is tightly bound by SutA under the condition tested. We also performed the experiment in reverse by immunoprecipitating RNAP from the same cell lysates with an anti-RpoA antibody and identifying coprecipitated proteins via LC-MS/MS. When coprecipitated proteins were ordered by total peptide intensities, HA-SutA ranked above known RNAP-binders σ^{70}, NusA, and Rho (Fig. S3 and Dataset S2).

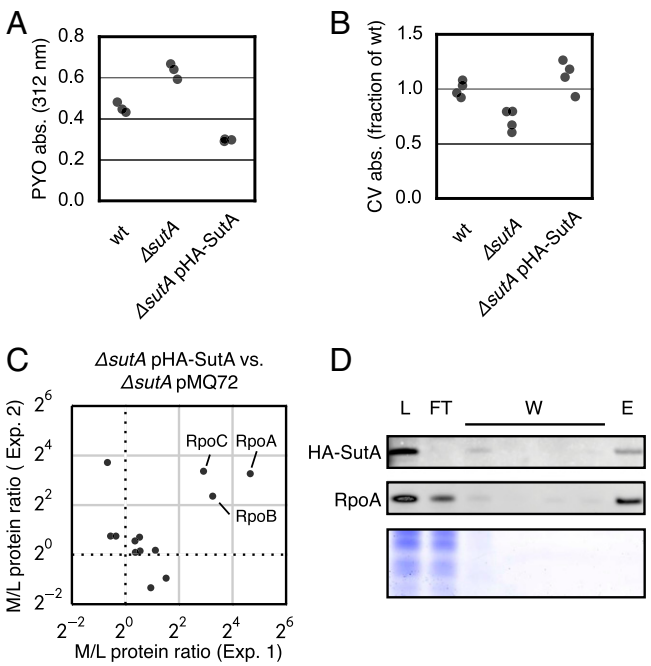

Fig. 4. RNA polymerase coprecipitates with SutA. (*A* and *B*) Absorbance measurements of culture supernatants (*A*) and crystal violet (CV) measurements (*B*) of biofilm formation. (*C*) LC-MS/MS detection and quantification of proteins coimmunoprecipitated with HA-SutA. Each axis represents the protein abundance ratio as determined by dimethyl quantification between proteins coprecipitated from the pHA-SutA [medium (M)] or pMQ72 control [light (L)] strains. The three main subunits of RNAP are indicated. (*D*) IP fractions were analyzed for the presence of HA-SutA and RpoA via Western blots and for total protein via Coomassie staining (*Lower*). E, eluent; FT, flow-through; L, lysate; W, washes.

SutA Associates with Genomic Loci and Enhances Transcription of Ribosomal Genes. To investigate the context of the interaction between SutA and RNAP and the effects this interaction might have on gene expression, we performed a chromatin IP (ChIP)-sequencing (Seq) experiment and an RNA-Seq experiment. The ChIP-Seq experiment was performed with the same strains and conditions used to detect the interaction with RNAP: the Δ*sutA* strain carrying HA-SutA on the pMQ72 arabinose-inducible plasmid and the Δ*sutA* strain carrying the pMQ72 empty vector as a control, both grown to late-exponential phase in pyruvate minimal medium in the presence of arabinose. We cross-linked protein–DNA complexes with formaldehyde, sonicated chromosomal DNA to generate fragments 0.5–1 kb in length, performed IPs against the HA epitope or against RpoA, and sequenced the coprecipitated DNA. For the RNA-Seq experiment, we sequenced rRNA-depleted RNA extracted from the wild-type, Δ*sutA*, and P_{ara}:*sutA* strains using the same growth medium and time point as for the ChIP-Seq experiment.

Because our IP experiment suggested that not all cellular RNAP was associated with SutA, we first sought to determine whether the interaction between SutA and RNAP occurs while RNAP is engaged in transcription, which should result in efficient formaldehyde cross-linking of SutA to genomic DNA, through concurrent interactions with RNAP. IP of HA-SutA led to an average recovery of 4% of input DNA compared with 0.2% in IPs from the empty vector control strain that did not encode HA-SutA (Fig. S4*A*), indicating that SutA likely interacts with RNAP while RNAP is interacting with genomic DNA. Over 1,400 of the ∼6,200 annotated genes showed a statistically significant enrichment in the HA-SutA IP compared with the empty vector IP, although the enrichment was greater than twofold for only 85 genes (Dataset S3). We next assessed the relationship between SutA and RNAP occupancies at genomic loci by comparing average per-gene reads per kilobase per million reads mapped (RPKM) from each IP. We saw a moderately strong correlation between the associations of SutA and RpoA across all genes (Fig. 5*A*; Pearson's $r = 0.77$), suggesting that SutA and RNAP tend to colocalize throughout the chromosome. This degree of correlation with RNAP ChIP signal is similar to what has been observed for NusG in *E. coli* ($r = 0.86$) and GreA in *Bacillus subtilis* ($r = 0.86$), both of which bind RNAP during transcription elongation (27, 28). When the ChIP data were divided into 100-bp tiles across the entire chromosome, the correlation between RNAP signal and HA-SutA signal had an r value of 0.66, which is lower than the value previously calculated in *E. coli* for DksA ($r = 0.79$) but higher than that for σ^{70} ($r = 0.57$), which dissociates from polymerase before transcription elongation (29). We noted that a subset of genes had ratios of SutA ChIP signal to RpoA ChIP signal that were substantially higher than the mean for all genes and found that many of these genes encoded ribosomal proteins (Fig. 5 *A* and *B*).

We next asked whether RNAP association at genomic loci was affected by the presence of SutA. We compared average per-gene ChIP signals for RpoA between the strain expressing HA-SutA and the strain carrying the empty vector. We found a very high correlation in per-gene RpoA ChIP signals between these two strains (Fig. S4*B*; Pearson's $r = 0.94$), suggesting that changes in the distribution of polymerase caused by the presence of SutA are subtle

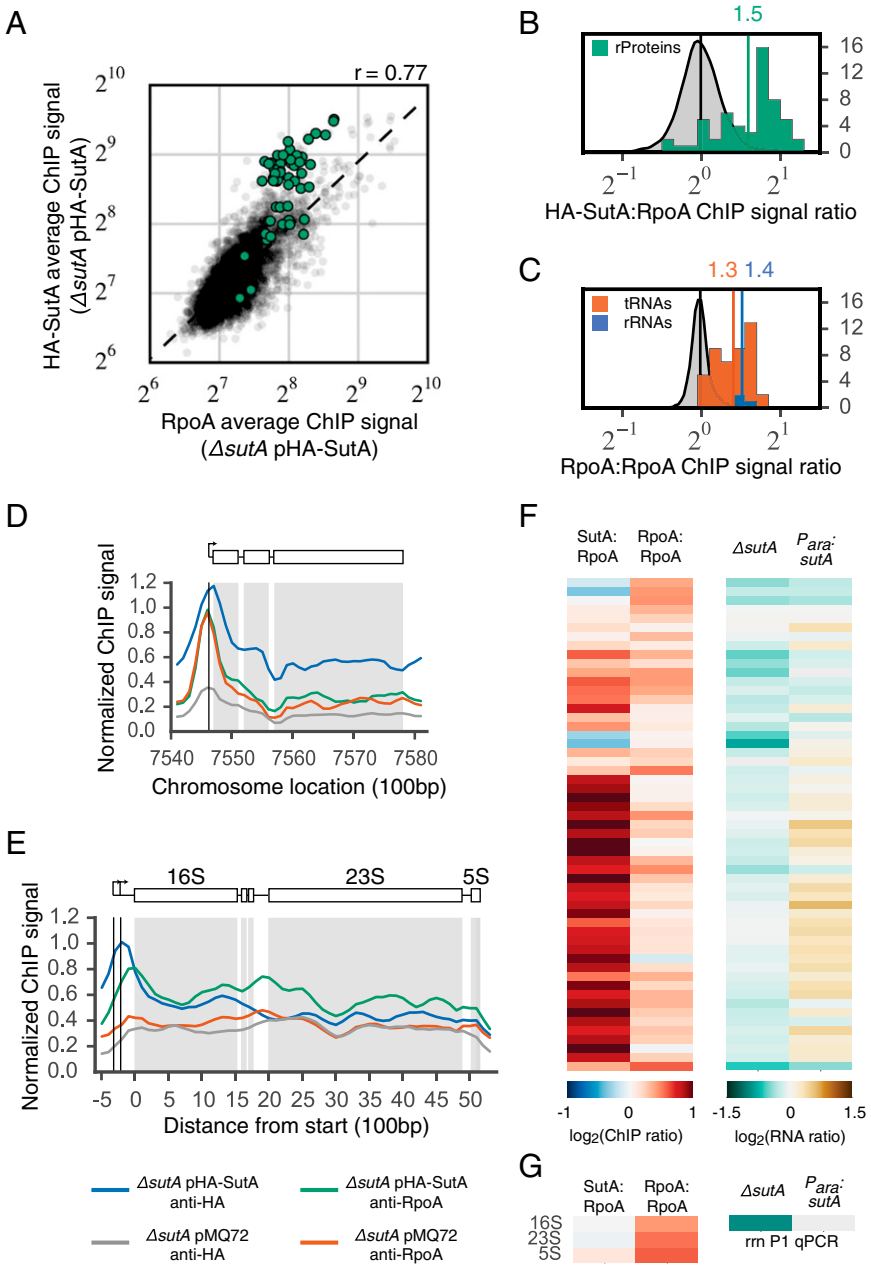

Fig. 5. SutA localizes throughout the chromosome and enhances transcription of ribosomal genes. (*A*) ChIP signals (RPKM) for HA-SutA vs. RpoA for each gene. Genes encoding ribosomal proteins are highlighted (green) (Pearson's $r = 0.77$). (*B*) Distribution of HA-SutA:RpoA ChIP signal ratios from the *ΔsutA* pHA-SutA strain for all genes (gray probability density plot) and for ribosomal protein genes (green histogram). (*C*) Distribution of the ratios of RpoA ChIP signal from *ΔsutA* pHA-SutA vs. *ΔsutA* pMQ72 for all genes (gray probability density plot), tRNAs (orange histogram), and rRNAs (blue histogram). The mean ratios for each subset are indicated above. (*D* and *E*) Normalized ChIP signals from each IP at the *rpsLG-fusA1* ribosomal protein operon (*D*) and for rRNA operons (*E*). (*E*, *Lower*) Legend describing strains and IPs for each trace. (*F* and *G*) Heat maps for ribosomal protein genes (*F*) and rRNA (*G*) showing ChIP signal ratios as calculated in *B* and *C* and transcript abundance ratios for *ΔsutA* and P_{ara}:*sutA* strains, each compared with the wild-type strain as determined by RNA-Seq (*F*) or qPCR (*G*).

or limited to a small number of loci. Although the differences in RPKM per gene were not statistically significant on an individual gene basis, we did note some departures from the overall high correlation. In particular, both rRNA and tRNA loci tended to show higher RpoA ChIP signals in the strain expressing HA-SutA compared with the strain lacking SutA (Fig. 5*C* and Fig. S4*D*).

To establish a higher-resolution view of SutA and RNAP associations at ribosomal protein and rRNA loci, we examined ChIP-Seq reads per 100-bp tile across the relevant loci. We adapted the "apparent occupancy" metric described previously for displaying ChIP-chip data (27). Because some nonspecific IP of DNA is expected, the normalized read counts observed at the least expressed genes in the genome were used to define a baseline signal representing no true occupancy, and the counts observed at the highest peaks in each sample that were associated with protein coding genes were used to define a maximum signal for that sample. All count values in each sample were then scaled from 0 to 1 based on the calculated baseline and maximum values for that sample. The count values for the IP from the empty vector strain are included for comparison and

are scaled to the baseline and maximum values calculated for the HA-SutA IP to best facilitate the comparison (the dynamic range for the empty vector IP was small, as expected for a control IP in which association is nonspecific) (see *SI Experimental Methods* and Datasets S4 and S5 for more information).

Ribosomal protein loci exhibited distinct peaks in RNAP and SutA signal near their transcription start sites (Fig. 5*D* and Fig. S4*C*). The SutA peak was shifted very slightly downstream from the RpoA peak, and the ratio of SutA signal to RpoA signal was high over promoter and coding regions, consistent with what was observed in the per-gene analysis. The presence of SutA did not result in a significant difference in RpoA signal at any individual ribosomal protein gene locus, but across all ribosomal protein genes, there appears to be a trend toward increased RpoA signal in the presence of SutA (Fig. 5*F*). Because the sequences of the four rRNA operons are nearly identical, these loci were aligned and the signals for homologous 100-bp tiles from each operon were averaged (Fig. 5*E*). Although the rRNA genes did not show high levels of HA-SutA ChIP signal relative to RpoA ChIP signal in our per-gene analysis, this higher-resolution view shows that a very strong peak of SutA signal is centered just upstream of the start of the 16S gene, near the predicted P2 transcription start site, with a lower ratio of SutA to RpoA signal across the coding region. This view also shows a statistically significant increase in the RpoA signal at the rRNA promoter region in the presence of SutA, which was missed in our per-gene analysis. These two features are distinct from the observations for the ribosomal protein loci.

We then investigated whether the presence of SutA at ribosomal protein and rRNA genomic loci, and the changes in RNAP localization to rRNA in particular, might impact their expression. To assess the effects of SutA on ribosomal protein gene mRNA levels, we queried our RNA-Seq dataset. We measured small but statistically significant differences in mRNA abundance among the three strains for a majority of the ribosomal protein genes [46 of 55 genes; false-discovery rate (FDR)-adjusted *P* value, <0.05] (Dataset S3). In general, ribosomal protein genes were expressed at higher levels in the P_{ara}:*sutA* strain, and at lower levels in the Δ*sutA* strain, compared with the wild-type strain (Fig. 5*F*). Because the stability of mature rRNA makes it a poor indicator of rRNA transcription rates, and because rRNA was intentionally depleted from our RNA-Seq samples before library construction, we used quantitative PCR (qPCR) against cDNA from the 16S leader sequence as a proxy for levels of new rRNA synthesis. The Δ*sutA* strain had levels of the 16S leader that were twofold lower compared with either the wild-type strain or the overexpression strain (Fig. 5*G* and Fig. S4*E*). Taken together, the ChIP and RNA abundance measurements suggest that the presence of SutA has a direct and positive effect on the transcription of both ribosomal protein and rRNA genes but that the nature of the interactions with these two types of loci may be distinct. Extensive work by many laboratories (reviewed in ref. 30) has shown that regulation of rRNA transcription occurs primarily at the level of initiation, whereas regulation of ribosomal protein gene transcription occurs mostly during elongation. Consistent with this regulatory paradigm, our ChIP data suggest association of SutA primarily in the promoter regions of rRNA genes but throughout the coding regions of ribosomal protein genes. Also potentially consistent with these two modes of regulation, we see a decrease in RpoA ChIP signal in the absence of SutA for rRNA genes but much less so for ribosomal protein genes. Further study will be required to elucidate the mechanistic details of these two possible regulatory modes.

SutA Localizes to Many Nonribosomal Genes and Has Broad Effects on Gene Expression. Ribosomal proteins and rRNAs are notable as classes of genes that had high levels of SutA association and whose transcript levels were significantly changed. However, the influence of SutA was not limited to these loci; much of the chromosome (~20% of all 100-bp regions) showed statistically significant enrichment for the HA-SutA IP compared with the empty vector IP. To explore the general pattern of association of SutA with genomic loci, we identified a "high ChIP signal" subset of 230 transcriptional units that (*i*) had high-quality peaks in both RpoA and SutA ChIP signals near their starts (defined as having an apparent occupancy greater than 0.25 for RpoA and 0.20 for SutA) and (*ii*) showed a statistically significant enrichment in the HA-SutA ChIP signal compared with the empty vector ChIP signal. For those that had annotated transcriptional start sites and were not among the ribosomal protein and RNA genes discussed above ($n = 171$), we averaged ChIP signal values

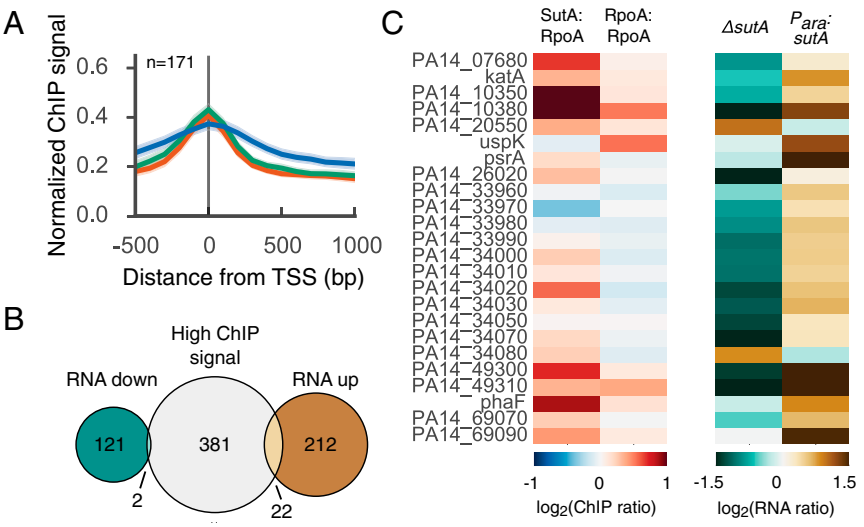

Fig. 6. SutA has broad effects on gene expression. (*A*) Average ChIP signals around transcriptional start sites (TSS) for genes in the high ChIP signal subset. Shaded regions around each trace represent the 95% confidence interval for the mean ($n = 171$). Traces represent the following: Δ*sutA* pHA-SutA, anti-HA (blue); Δ*sutA* pHA-SutA, anti-RpoA (green); and Δ*sutA* pMQ72, anti-RpoA (orange). The direction of transcription is from left to right. (*B*) Numbers of genes in the high ChIP signal subset and genes whose expression changed more than twofold between the Δ*sutA* and P_{ara}:*SutA* strains. (*C*) Heat maps (as in Fig. 5 *F* and *G*) for genes found in both subsets.

from 500 bp upstream to 1,000 bp downstream of that location to generate aggregate traces of the associations of RNAP and HA-SutA across nonribosomal loci (Fig. 6*A*). The average pattern of RpoA and SutA association across these transcriptional units was similar to that observed for the ribosomal protein genes: RpoA association was centered at the transcriptional start site and a broader peak of HA-SutA was centered slightly downstream. This aggregate includes upstream regions that drive transcription of diverging transcription units as well as those for which adjacent transcription units are on the same strand, so the breadth of the observed peaks may reflect limits of the resolution of our ChIP technique as well as contributions from binding to adjacent transcriptional units.

We next investigated whether SutA association at nonribosomal transcriptional units was also associated with increased expression. To focus on likely direct effects, we examined the 24 genes that were among the high ChIP signal subset and also showed greater than twofold changes in transcript levels; 22 of these genes (92%) had higher transcript levels in the overexpression strain than in the deletion strain (Fig. 6 *B* and *C*), suggesting, as was observed for the ribosomal protein and rRNA genes, that the presence of SutA at these genomic loci tends to enhance their transcription. Higher-resolution views of specific loci reinforced the observations from the aggregate analysis: transcription units exhibited a broad peak of HA-SutA association centered downstream of the peak of RpoA association. PA14_10380 is predicted to encode a protein that is structurally similar to bacteriocins and is among the highest ranked-genes both in terms of SutA association and differential expression between the Δ*sutA* and the P_{ara}:*sutA* strains (Fig. S4*F*) (31). PA14_21220 encodes the universal stress protein UspK (Fig. S4*G*), and PA14_26020 encodes an aminopeptidase (Fig. S4*H*). In each of these cases, the apparent occupancy of RpoA in the promoter region is higher in the SutA-containing strain.

Many of the genes that were differentially expressed in the SutA mutants were not among the genes that showed the highest ChIP signal, and many genes that had high ChIP signal did not show large SutA-dependent changes in gene expression (Fig. 6*B*). This pattern is likely attributable to several factors. First, because the presence of SutA generally enhances transcription at loci to which it is recruited, decreased expression in the presence of SutA may be attributable largely to the shift of free RNAP to highly expressed loci that are up-regulated by SutA (e.g., rRNA). Our data show several transcriptional units that recruit significantly more RNAP in the absence of SutA (as evidenced by higher RpoA ChIP peaks in the strain lacking HA-SutA and no significant SutA association in the HA-SutA ChIP experiment) and that have increased expression in the Δ*sutA* strain; PA14_40800 and PA14_40100-40110, divergently transcribed, are two examples (Fig. S4*I*). Second, the list of genes that are likely directly regulated by SutA includes the components of the ribosome as well as known master regulators such as the stationary-phase transcription factor *psrA* (32). Increased expression of these genes is likely to cause widespread secondary effects, which may explain why some genes that are up-regulated in the presence of SutA do not show strong HA-SutA ChIP signal. Third, as suggested by our analysis of rRNA and ribosomal protein genes, SutA may affect different aspects of transcription for different genes (e.g., initiation vs. elongation), with different patterns of ChIP signals and expression levels resulting. Further work is required to fully understand the impacts of SutA on different genes and different phases of gene expression.

Finally, to take a broad view of the effects of SutA, both direct and indirect, on the physiological state of the cell, we grouped the genes that differed more than twofold between the Δ*sutA* and the P_{ara}:*sutA* strains according to their functional designations from the Clusters of Orthologous Groups (COG) categories (33) and asked whether any groups were differentially represented compared with the genome as a whole (Fig. S4*J*). In general, genes that were up-regulated in the presence of SutA tended to have functions related to energy generation and maintenance; these genes included proteases, oxidoreductases, and alternate metabolism genes. Conversely, genes involved in growth and carbohydrate and amino acid metabolism were significantly underrepresented. Genes that were down-regulated were more likely to be involved in defense mechanisms, signaling, and motility. For the full set of results, see Dataset S3 and GEO accession no. GSE66181.

Discussion

Although microbes have spent the majority of their evolutionary history enduring slow-growth conditions, relatively little is known about their physiology in these states. In part, this knowledge gap arises from technical challenges—slow metabolic rates and high phenotypic heterogeneity can lead to increased noise and decreased signal for many biomolecules of interest. However, slow-growth and survival states are of great relevance in many clinical and environmental contexts, and new tools are needed for their study. As illustrated here, the BONCAT method, which enables enrichment of newly synthesized proteins from large preexisting proteomes, is well suited to the exploration of slow-growth modes of microbial life.

We used the BONCAT method to discover a previously unknown RNAP-binding factor, which we have named SutA. We found SutA to be up-regulated posttranscriptionally in various growth-limiting conditions. Through its interaction with RNAP, SutA localizes to many genes throughout the chromosome and elicits broad transcriptional changes. Some of these changes are likely direct effects; for example, SutA associates strongly with loci encoding ribosomal components, and the transcription of these loci is reduced in the absence of SutA. Other changes may be attributable to secondary effects resulting from changes in the pool of free polymerase or from changes in downstream regulation by directly affected genes. Our broad analysis of transcriptional changes suggests that cells expressing SutA prioritize the expression of genes required for survival, and our phenotypic studies show that SutA is important for the establishment of biofilms, the regulation of phenazine production, and transitions to and from growth-limited states.

Understanding the molecular mechanism by which SutA effects these changes will require further study, but our observations suggest some intriguing comparisons to the well-studied regulator DksA. DksA acts with the small molecule alarmone ppGpp during nutritional downshifts to destabilize open promoter complexes, especially at rRNA promoters. This activity reduces rRNA transcription in response to a decreased availability of nucleotides (34). DksA may also influence elongation by helping to prevent the transition of RNAP from a paused to an arrested state (35). Interestingly, SutA appears to affect many of the same genes and phenotypes as DksA but in the opposite direction. Whereas DksA has been shown in both *E. coli* and *P. aeruginosa* to repress expression of ribosomal protein and rRNA genes (34, 36, 37), SutA enhances expression of these genes. Both DksA and SutA show high ChIP signal across the coding regions of highly expressed protein-coding genes, including ribosomal protein genes, and a lower signal across the coding regions of the rRNA genes. However, unlike DksA, SutA shows a high peak of ChIP signal at the promoters of rRNA genes, consistent with the observations that SutA enhances rRNA expression, whereas DksA represses rRNA expression (29). Disruptions of *dksA* or *sutA* in *Pseudomonas* species also appear to cause opposing phenotypes: disruption of *dksA* causes a decrease in PYO production and an increase in biofilm persistence (38, 39), whereas deletion of *sutA* causes overproduction of PYO and a decrease in biofilm accumulation. Taken together, these observations suggest that a subset of genes, including the rRNA and ribosomal protein genes, are sensitive to some modulation of RNAP activity, and DksA and SutA tend to modulate this activity in opposite ways.

In our BONCAT experiment, we detected new synthesis of DksA in the aerobic exponential growth condition but not in the anaerobic survival condition. This finding is consistent with a previous report that DksA is undetectable by Western blot during stationary phase in *P. aeruginosa* (36) and suggests that the repression by DksA of rRNA and ribosomal protein gene expression is down-regulated during protracted slow growth. DksA is advantageous in the context of actively growing cells because it protects against "traffic jams" of stalled RNAP that obstruct the completion of DNA replication (40) and allows limited cellular resources to be directed toward expression of genes important for ameliorating the limitations (e.g., amino acid biosynthetic genes) (41). However, for cells that are dividing infrequently or not at all, and that are limited for basic energy resources rather than specific metabolites, these functions may be counterproductive. Instead, the most adaptive response may be to maintain transcription, even at low levels, of core machinery to retain a capacity for cellular maintenance and to allow for a rapid up-regulation of biosynthetic pathways when conditions improve. Our results suggest that SutA contributes to this type of response, and set the stage for future biochemical and structural studies.

Recent reports have described RNAP-binding regulators that broadly affect transcription in different organisms under a range of conditions, suggesting that this is an important and diverse mode of regulation. For example, the nonessential δ subunit of *B. subtilis* RNAP (42) and the recently discovered AtfA from *Acinetobacter* spp. (43) are both small proteins that, like SutA, contain highly acidic domains and broadly impact transcription but, unlike SutA, are expressed during exponential phase. CarD is a mycobacterial protein that has recently been crystallized in a complex with RNAP; unlike SutA, CarD is essential and appears to localize primarily to promoter regions, but like SutA it broadly serves to stimulate transcription. One characteristic of all of these proteins is that they lack homologs in *E. coli*, the model organism from which much of our knowledge of bacterial transcriptional regulatory mechanisms has been derived. Each protein has a different phylogenetic distribution; SutA is found only in selected families of the Alteromonadales and Pseudomonadales orders of Gammaproteobacteria. This growing body of work, including the results described here, demonstrates that regulation of RNAP is diverse, and even in well-studied, clinically important pathogens, basic regulatory mechanisms governing slow growth remain to be discovered.

Experimental Procedures

For detailed descriptions of all experimental procedures, see *SI Experimental Procedures*. The strains and plasmids used are listed in Table S1.

Strains and Growth Conditions. Rich medium was LB broth. Minimal medium was phosphate-buffered and contained 40 mM carbon source (10). In experiments involving P_{ara}:*sutA*, all cultures were grown in the presence of 20–25 mM arabinose. Where necessary, plasmids were maintained with the appropriate antibiotics. Aerobic growth was carried out with shaking at 37 °C. Anaerobic survival was carried out in Balch tubes in an anaerobic chamber (Coy) without shaking at 37 °C. Growth for colony morphology assays was carried out at room temperature. Genetic manipulations used standard procedures.

Biofilm Measurements. Crystal violet and colony morphology assays were carried out as previously described (44, 45).

Phenazine Measurements. Phenazine concentrations in culture supernatants were determined by HPLC as previously described (23) or estimated by measuring absorbance at 312 nm.

Individual Gene Expression Measurements. Per-cell GFP measurements were made using the Accuri c6 flow cytometer, and RNA measurements were made by qPCR. Primers are listed in Table S2.

Proteomics. BONCAT labeling, chemistry, and enrichment were performed as previously described (46). Label-free quantitation was used for the initial screen. Relative protein abundances for IPs were quantified via dimethyl labeling (47).

IP and ChIP. Cultures of *ΔsutA* pMQ72 or *ΔsutA* pMQ72-HA-SutA were grown to late-exponential phase in pyruvate minimal medium containing 20 mM arabinose and 50 μg/mL gentamicin. HA-SutA or RpoA was purified with anti-HA agarose beads (Thermo Fisher Scientific) or protein A/G beads (Santa Cruz Biotechnology) and an anti-RpoA antibody, respectively. Fractions were saved for Western blot analysis, and eluents were analyzed via LC-MS/MS. For ChIP, cultures were grown as above, cross-linked with 1% formaldehyde, and lysed via sonication, and either HA-SutA or RpoA was immunoprecipitated. Protein digestion and DNA cleanup were performed as previously described (48).

Sequencing Library Preparation and Sequencing. For RNA-Seq, cultures of wild-type, *ΔsutA*, and P_{ara}:*sutA* strains were grown to late-exponential phase in pyruvate minimal medium containing 25 mM arabinose. Total RNA was extracted using the RNeasy Mini Kit (Qiagen), and rRNA was depleted using the Magnetic Gram Negative Bacteria RiboZero Kit (Epicentre). For ChIP-Seq, immunoprecipitated DNA was further fragmented using DS Fragmentase (NEB). Both types of libraries were prepared using the relevant Library Prep kits for Illumina (NEB). Sequencing was performed to a depth of 10–15 million reads per sample on an Illumina HiSeq2500 machine, and data analysis was performed using standard open source software, or as described in more detail in *SI Experimental Procedures*. Sequencing was performed on biological triplicates.

ACKNOWLEDGMENTS. We thank Geoff Smith and Roxana Eggleston-Rangel for technical assistance with liquid chromatography–tandem mass spectrometry and Dr. Igor Antoshechkin for assistance with sequencing. We thank Dr. Olaf Schneewind for his gift of the anti-RpoA antibody. We appreciate constructive feedback on the manuscript from members of the D.K.N. and D.A.T. laboratories and Richard Gourse, as well as helpful comments from the editor and reviewers. This work was supported by NIH Grants 5R01HL117328-03 (to D.K.N.) and 1S10RR029594-01A1 (to S.H.), the Institute for Collaborative Biotechnologies through US Army Research Office Grant W911NF-09-0001 (to D.A.T.), Howard Hughes Medical Institute (HHMI), and the Millard and Muriel Jacobs Genetics and Genomics Laboratory at California Institute of Technology (Caltech). The Proteome Exploration Laboratory (M.J.S., A.M., and S.H.) was supported by Gordon and Betty Moore Foundation Grant GBMF775 and by the Beckman Institute at Caltech. D.K.N. is an HHMI Investigator.

1. Stover CK, et al. (2000) Complete genome sequence of *Pseudomonas aeruginosa* PAO1, an opportunistic pathogen. *Nature* 406(6799):959–964.
2. Potvin E, Sanschagrin F, Levesque RC (2008) Sigma factors in *Pseudomonas aeruginosa*. *FEMS Microbiol Rev* 32(1):38–55.
3. Salgado H, et al. (2006) RegulonDB (version 5.0): *Escherichia coli* K-12 transcriptional regulatory network, operon organization, and growth conditions. *Nucleic Acids Res* 34(Database issue):D394–D397.
4. Wurtzel O, et al. (2012) The single-nucleotide resolution transcriptome of *Pseudomonas aeruginosa* grown in body temperature. *PLoS Pathog* 8(9):e1002945.
5. Raghavan R, Groisman EA, Ochman H (2011) Genome-wide detection of novel regulatory RNAs in *E. coli*. *Genome Res* 21(9):1487–1497.
6. Kopf SH, et al. Trace incorporation of heavy water reveals slow and heterogeneous pathogen growth rates in cystic fibrosis sputum. *Proc Natl Acad Sci USA* 113(2):E110–E116.
7. Cowley ES, Kopf SH, LaRiviere A, Ziebis W, Newman DK (2015) Pediatric cystic fibrosis sputum can be chemically dynamic, anoxic, and extremely reduced due to hydrogen sulfide formation. *MBio* 6(4):e00767.
8. Hoboth C, et al. (2009) Dynamics of adaptive microevolution of hypermutable *Pseudomonas aeruginosa* during chronic pulmonary infection in patients with cystic fibrosis. *J Infect Dis* 200(1):118–130.
9. Quinn RA, et al. (2014) Biogeochemical forces shape the composition and physiology of polymicrobial communities in the cystic fibrosis lung. *MBio* 5(2):e00956-13.
10. Glasser NR, Kern SE, Newman DK (2014) Phenazine redox cycling enhances anaerobic survival in *Pseudomonas aeruginosa* by facilitating generation of ATP and a protonmotive force. *Mol Microbiol* 92(2):399–412.
11. Eschbach M, et al. (2004) Long-term anaerobic survival of the opportunistic pathogen *Pseudomonas aeruginosa* via pyruvate fermentation. *J Bacteriol* 186(14):4596–4604.
12. Vander Wauven C, Piérard A, Kley-Raymann M, Haas D (1984) *Pseudomonas aeruginosa* mutants affected in anaerobic growth on arginine: Evidence for a four-gene cluster encoding the arginine deiminase pathway. *J Bacteriol* 160(3):928–934.
13. Alvarez-Ortega C, Harwood CS (2007) Responses of *Pseudomonas aeruginosa* to low oxygen indicate that growth in the cystic fibrosis lung is by aerobic respiration. *Mol Microbiol* 65(1):153–165.

14. Trunk K, et al. (2010) Anaerobic adaptation in *Pseudomonas aeruginosa*: Definition of the Anr and Dnr regulons. *Environ Microbiol* 12(6):1719–1733.
15. Schreiber K, et al. (2006) Anaerobic survival of *Pseudomonas aeruginosa* by pyruvate fermentation requires an Usp-type stress protein. *J Bacteriol* 188(2):659–668.
16. Repoila F, Majdalani N, Gottesman S (2003) Small non-coding RNAs, co-ordinators of adaptation processes in *Escherichia coli*: The RpoS paradigm. *Mol Microbiol* 48(4): 855–861.
17. Storz G, Vogel J, Wassarman KM (2011) Regulation by small RNAs in bacteria: Expanding frontiers. *Mol Cell* 43(6):880–891.
18. Dieterich DC, et al. (2007) Labeling, detection and identification of newly synthesized proteomes with bioorthogonal non-canonical amino-acid tagging. *Nat Protoc* 2(3): 532–540.
19. Dieterich DC, Link AJ, Graumann J, Tirrell DA, Schuman EM (2006) Selective identification of newly synthesized proteins in mammalian cells using bioorthogonal noncanonical amino acid tagging (BONCAT). *Proc Natl Acad Sci USA* 103(25): 9482–9487.
20. Liberati NT, et al. (2006) An ordered, nonredundant library of *Pseudomonas aeruginosa* strain PA14 transposon insertion mutants. *Proc Natl Acad Sci USA* 103(8): 2833–2838.
21. Stewart PS, Franklin MJ (2008) Physiological heterogeneity in biofilms. *Nat Rev Microbiol* 6(3):199–210.
22. Michel GPF, et al. (2011) Role of fimV in type II secretion system-dependent protein secretion of *Pseudomonas aeruginosa* on solid medium. *Microbiology* 157(Pt 7): 1945–1954.
23. Dietrich LE, Price-Whelan A, Petersen A, Whiteley M, Newman DK (2006) The phenazine pyocyanin is a terminal signalling factor in the quorum sensing network of *Pseudomonas aeruginosa*. *Mol Microbiol* 61(5):1308–1321.
24. Lau GW, Hassett DJ, Ran H, Kong F (2004) The role of pyocyanin in *Pseudomonas aeruginosa* infection. *Trends Mol Med* 10(12):599–606.
25. Wang Y, Kern SE, Newman DK (2010) Endogenous phenazine antibiotics promote anaerobic survival of *Pseudomonas aeruginosa* via extracellular electron transfer. *J Bacteriol* 192(1):365–369.
26. Fröhlich KS, Vogel J (2009) Activation of gene expression by small RNA. *Curr Opin Microbiol* 12(6):674–682.
27. Mooney RA, et al. (2009) Regulator trafficking on bacterial transcription units in vivo. *Mol Cell* 33(1):97–108.
28. Kusuya Y, Kurokawa K, Ishikawa S, Ogasawara N, Oshima T (2011) Transcription factor GreA contributes to resolving promoter-proximal pausing of RNA polymerase in *Bacillus subtilis* cells. *J Bacteriol* 193(12):3090–3099.
29. Zhang Y, et al. (2014) DksA guards elongating RNA polymerase against ribosome-stalling-induced arrest. *Mol Cell* 53(5):766–778.
30. Dennis PP, Ehrenberg M, Bremer H (2004) Control of rRNA synthesis in *Escherichia coli*: A systems biology approach. *Microbiol Mol Biol Rev* 68(4):639–668.
31. Michiels J, Dirix G, Vanderleyden J, Xi C (2001) Processing and export of peptide pheromones and bacteriocins in Gram-negative bacteria. *Trends Microbiol* 9(4): 164–168.
32. Kang Y, et al. (2009) The long-chain fatty acid sensor, PsrA, modulates the expression of rpoS and the type III secretion exsCEBA operon in *Pseudomonas aeruginosa*. *Mol Microbiol* 73(1):120–136.
33. Tatusov RL, et al. (2003) The COG database: An updated version includes eukaryotes. *BMC Bioinformatics* 4:41.
34. Paul BJ, et al. (2004) DksA: A critical component of the transcription initiation machinery that potentiates the regulation of rRNA promoters by ppGpp and the initiating NTP. *Cell* 118(3):311–322.
35. Perederina A, et al. (2004) Regulation through the secondary channel–structural framework for ppGpp-DksA synergism during transcription. *Cell* 118(3):297–309.
36. Perron K, Comte R, van Delden C (2005) DksA represses ribosomal gene transcription in *Pseudomonas aeruginosa* by interacting with RNA polymerase on ribosomal promoters. *Mol Microbiol* 56(4):1087–1102.
37. Lemke JJ, et al. (2011) Direct regulation of *Escherichia coli* ribosomal protein promoters by the transcription factors ppGpp and DksA. *Proc Natl Acad Sci USA* 108(14): 5712–5717.
38. Blaby-Haas CE, Furman R, Rodionov DA, Artsimovitch I, de Crécy-Lagard V (2011) Role of a Zn-independent DksA in Zn homeostasis and stringent response. *Mol Microbiol* 79(3):700–715.
39. López-Sánchez A, Jiménez-Fernández A, Calero P, Gallego LD, Govantes F (2013) New methods for the isolation and characterization of biofilm-persistent mutants in *Pseudomonas putida*. *Environ Microbiol Rep* 5(5):679–685.
40. Tehranchi AK, et al. (2010) The transcription factor DksA prevents conflicts between DNA replication and transcription machinery. *Cell* 141(4):595–605.
41. Gummesson B, Lovmar M, Nyström T (2013) A proximal promoter element required for positive transcriptional control by guanosine tetraphosphate and DksA protein during the stringent response. *J Biol Chem* 288(29):21055–21064.
42. López de Saro FJ, Woody AY, Helmann JD (1995) Structural analysis of the *Bacillus subtilis* delta factor: A protein polyanion which displaces RNA from RNA polymerase. *J Mol Biol* 252(2):189–202.
43. Withers R, et al. (2014) AtfA, a new factor in global regulation of transcription in *Acinetobacter spp*. *Mol Microbiol* 93(6):1130–1143.
44. Dietrich LE, et al. (2013) Bacterial community morphogenesis is intimately linked to the intracellular redox state. *J Bacteriol* 195(7):1371–1380.
45. Müsken M, Di Fiore S, Dötsch A, Fischer R, Häussler S (2010) Genetic determinants of *Pseudomonas aeruginosa* biofilm establishment. *Microbiology* 156(Pt 2):431–441.
46. Mahdavi A, et al. (2014) Identification of secreted bacterial proteins by noncanonical amino acid tagging. *Proc Natl Acad Sci USA* 111(1):433–438.
47. Boersema PJ, Raijmakers R, Lemeer S, Mohammed S, Heck AJ (2009) Multiplex peptide stable isotope dimethyl labeling for quantitative proteomics. *Nat Protoc* 4(4):484–494.
48. Gilbert KB, Kim TH, Gupta R, Greenberg EP, Schuster M (2009) Global position analysis of the *Pseudomonas aeruginosa* quorum-sensing transcription factor LasR. *Mol Microbiol* 73(6):1072–1085.
49. Shanks RM, Caiazza NC, Hinsa SM, Toutain CM, O'Toole GA (2006) *Saccharomyces cerevisiae*-based molecular tool kit for manipulation of genes from gram-negative bacteria. *Appl Environ Microbiol* 72(7):5027–5036.
50. Choi KH, Schweizer HP (2006) mini-Tn7 insertion in bacteria with single attTn7 sites: Example *Pseudomonas aeruginosa*. *Nat Protoc* 1(1):153–161.
51. Gibson DG (2011) Enzymatic assembly of overlapping DNA fragments. *Methods Enzymol* 498:349–361.
52. Fong JC, Karplus K, Schoolnik GK, Yildiz FH (2006) Identification and characterization of RbmA, a novel protein required for the development of rugose colony morphology and biofilm structure in *Vibrio cholerae*. *J Bacteriol* 188(3):1049–1059.
53. Pédelacq JD, Cabantous S, Tran T, Terwilliger TC, Waldo GS (2006) Engineering and characterization of a superfolder green fluorescent protein. *Nat Biotechnol* 24(1): 79–88.
54. Link AJ, Vink MK, Tirrell DA (2007) Preparation of the functionalizable methionine surrogate azidohomoalanine via copper-catalyzed diazo transfer. *Nat Protoc* 2(8): 1879–1883.
55. Szychowski J, et al. (2010) Cleavable biotin probes for labeling of biomolecules via azide-alkyne cycloaddition. *J Am Chem Soc* 132(51):18351–18360.
56. Hong V, Presolski SI, Ma C, Finn MG (2009) Analysis and optimization of copper-catalyzed azide-alkyne cycloaddition for bioconjugation. *Angew Chem Int Ed Engl* 48(52):9879–9883.
57. Rappsilber J, Mann M, Ishihama Y (2007) Protocol for micro-purification, enrichment, pre-fractionation and storage of peptides for proteomics using StageTips. *Nat Protoc* 2(8):1896–1906.
58. Kalli A, Hess S (2012) Effect of mass spectrometric parameters on peptide and protein identification rates for shotgun proteomic experiments on an LTQ-orbitrap mass analyzer. *Proteomics* 12(1):21–31.
59. Cox J, Mann M (2008) MaxQuant enables high peptide identification rates, individualized p.p.b.-range mass accuracies and proteome-wide protein quantification. *Nat Biotechnol* 26(12):1367–1372.
60. Bagert JD, et al. (2014) Quantitative, time-resolved proteomic analysis by combining bioorthogonal noncanonical amino acid tagging and pulsed stable isotope labeling by amino acids in cell culture. *Mol Cell Proteomics* 13(5):1352–1358.
61. Bolger AM, Lohse M, Usadel B (2014) Trimmomatic: A flexible trimmer for Illumina sequence data. *Bioinformatics* 30(15):2114–2120.
62. Langmead B, Trapnell C, Pop M, Salzberg SL (2009) Ultrafast and memory-efficient alignment of short DNA sequences to the human genome. *Genome Biol* 10(3):R25.
63. Li H, et al. (2009) The sequence alignment/map format and SAMtools. *Bioinformatics* 25(16):2078–2079.
64. Delhomme N, Padioleau I, Furlong EE, Steinmetz LM (2012) easyRNASeq: A bioconductor package for processing RNA-Seq data. *Bioinformatics* 28(19):2532–2533.
65. Law CW, Chen Y, Shi W, Smyth GK (2014) voom: Precision weights unlock linear model analysis tools for RNA-seq read counts. *Genome Biol* 15(2):R29.
66. Homann OR, Johnson AD (2010) MochiView: Versatile software for genome browsing and DNA motif analysis. *BMC Biol* 8:49.
67. Winsor GL, et al. (2011) Pseudomonas Genome Database: Improved comparative analysis and population genomics capability for *Pseudomonas* genomes. *Nucleic Acids Res* 39(Database issue):D596–D600.
68. Hunter JD (2007) Matplotlib: A 2D graphics environment. *Comput Sci Eng* 9(3):90–95.
69. Schneider CA, Rasband WS, Eliceiri KW (2012) NIH Image to ImageJ: 25 years of image analysis. *Nat Methods* 9(7):671–675.